

Cite this: *Chem. Sci.*, 2018, **9**, 4275

## Long-lived protein expression in hydrogel particles: towards artificial cells†

Xiaoyu Zhou, Han Wu, Miao Cui, Sze Nga Lai and Bo Zheng  \*

Herein we report a new type of cell-mimic particle capable of long-lived protein expression. We constructed the cell-mimic particles by immobilizing the proteinaceous factors of the cell-free transcription and translation system on the polymer backbone of hydrogel particles and encapsulating the plasmid template and ribosome inside the hydrogel. With the continuous supply of nutrients and energy, the protein expression in the cell-mimic particles remained stable for at least 11 days. We achieved the regulation of protein expression in the cell-mimic particles by the usage of lac operon. The cell-mimic particles quickly responded to the concentration change of isopropyl  $\beta$ -D-1-thiogalactopyranoside (IPTG) in the feeding buffer to regulate the mCherry expression level. We also constructed an *in vitro* genetic oscillator in the cell-mimic particles. Protein LacI provided a negative feedback to the expression of both LacI itself and eGFP, and the expression level change of eGFP presented an oscillation. We expect the cell-mimic particles to be a useful platform for gene circuit engineering, metabolic engineering, and biosensors.

Received 23rd January 2018

Accepted 14th April 2018

DOI: 10.1039/c8sc00383a

rsc.li/chemical-science

## Introduction

Artificial cells are an essential tool in the research of the origin of life,<sup>1–4</sup> synthetic biology,<sup>5–7</sup> drug delivery,<sup>8–11</sup> gene therapy,<sup>12,13</sup> etc. Artificial cells are generally capable of some functions or behaviors of natural cells, such as protein expression,<sup>14–17</sup> communication,<sup>18–21</sup> and self-replication.<sup>1,22</sup> These artificial cells are mostly liposomes,<sup>23,24</sup> polymersomes,<sup>25,26</sup> hydrogels,<sup>27,28</sup> or simply aqueous droplets<sup>29</sup> encapsulating the cell-free expression system. Cell-free expression systems are usually cell extracts from *Escherichia coli* (*E. coli*), wheat embryo and rabbit reticulocytes<sup>30,31</sup> supplemented with energy components and free amino acids.<sup>32–34</sup> In addition, a purified cell-free transcription and translation system, termed the protein synthesis using recombinant elements (PURE) system was developed by Ueda and co-workers.<sup>35</sup> The PURE system was reconstituted from the essential elements of the *E. coli* transcription and translation system.

Cell-free protein expression in an artificial cell in the batch format mostly terminated within a few hours due to the depletion of energy and nutrients and the accumulation of waste products.<sup>33,35</sup> To solve this problem, many efforts were devoted to building artificial cells capable of long-lived protein expression through continuous energy and nutrient uptake and waste elimination. Dialysis membranes encapsulating the cell-

free protein expression system inside were introduced, and the protein expression in the artificial cells could last tens of hours with higher protein yield.<sup>14</sup> However, dialysis membranes presented a molecular weight cut-off, making it difficult for macromolecules including protein products to pass through the pores. Recently, Maerkl and co-workers built a micro-reactor that supported regulated protein expression up to 30 hours.<sup>36</sup> Mass exchange and mixing were actively controlled by the integrated pneumatic valves. Noireaux *et al.* reported vesicle-based artificial cells which expressed and anchored the pore proteins to the vesicle membrane.<sup>37</sup> Small molecules such as the energy source and nutrients can diffuse through the nanopores in the membrane, thus facilitating continuous protein expression up to 4 days. However, vesicle-based artificial cells required a delicate balance of osmotic pressure to prevent vesicle bursting. In contrast to the microencapsulation of the cell free expression system, micro-compartmentation of DNA templates, *e.g.*, DNA gel<sup>27</sup> and DNA brushes,<sup>21,38</sup> allowed continuous protein expression when the cell free expression system was supplied together with energy and nutrients. DNA brush based artificial cells provide a useful platform for studying synthetic networks.<sup>21</sup> However, DNA brushes present characteristics more of a biochip than an artificial cell, and functions such as multi-compartments, motility and chemotaxis<sup>39</sup> are difficult to achieve.

Herein, we aimed to construct hydrogel-based cell-mimic particles capable of long-lived protein expression. Instead of physical entrapment of the transcription and translation system in polymeric particles as in previous studies<sup>40–42</sup> to achieve cell-free protein expression, we immobilized the proteinaceous factors of the PURE system on the polymer backbone of

Department of Chemistry, The Chinese University of Hong Kong, Shatin, Hong Kong, P. R. China. E-mail: bozheng@cuhk.edu.hk

† Electronic supplementary information (ESI) available: Experimental details and results. See DOI: 10.1039/c8sc00383a

hydrogel particles through chelating bonds. We achieved selective nutrient, waste, and energy exchange by the diffusion process between the surrounding buffer and the cell-mimic particles. The resulting cell-mimic particles were an open system that supported not only long-lived protein expression, but also expression regulation and genetic oscillators.

## Results and discussion

We first prepared a functionalized polyacrylamide (PA) hydrogel that presented a nickel(II)-nitrilotriacetic acid ( $\text{Ni}^{2+}$ -NTA) moiety on the polymer backbone (Fig. 1a). First, acrylic acid *N*-hydroxysuccinimide ester was copolymerized with the hydrogel precursors. Then *N,N*-bis(carboxymethyl)-L-lysine hydrate (AB-NTA) was incorporated into the polymer backbone through the reaction with the *N*-hydroxysuccinimide (NHS) group. After the formation of the  $\text{Ni}^{2+}$ -NTA complex, the resulting functionalized PA hydrogel can be used for the immobilization of His-tagged proteins.<sup>43</sup> We evaluated the immobilization efficiency of the functionalized hydrogel by using the His-tagged eGFP. The PA hydrogel particles were treated with the solution of His-tagged eGFP, followed by washing with water several times. A control experiment was performed by treating the unfunctionalized PA hydrogel with the same solution of His-tagged eGFP. The His-tagged eGFP remained in the functionalized PA hydrogel after washing with water (Fig. 1b and c), on the other hand, the His-tagged eGFP in the functionalized PA hydrogel could be washed away with imidazole (Fig. 1d), further indicating that the His-tagged eGFP was immobilized through the interaction between the His-tag and the  $\text{Ni}^{2+}$ -NTA complex.

We started the construction of cell-mimic particles by preparing uniform functionalized PA hydrogel particles with

a size of 50  $\mu\text{m}$  using the microfluidic T-junction platform.<sup>44</sup> The hydrogel particles were heated in air at 100 °C to be dehydrated. The PURE system proteinaceous factors, ribosome and plasmid templates were loaded into the PA hydrogel particles when the predried PA hydrogel particles were rehydrated in the PURE system solution.<sup>45</sup> The enzyme mixture of the PURE system includes 20 tRNA synthetases, 3 initiation factors (IF1, IF2, and IF3), 3 elongation factors (EF-G, EF-Tu, and EF-Ts), 3 release factors (RF1, RF2, and RF3), ribosome recycling factor, myokinase, creatine kinase, nucleoside-diphosphate kinase, peptidylprolyl-isomerase, T7 RNA polymerase, and 70S ribosome. The proteinaceous factors of the PURE system were all labelled with the His-tag and immobilized through the interaction of the His-tag and the  $\text{Ni}^{2+}$ -NTA complex. The ribosomes were non-His-tagged with a relatively large size of around 20 nm, while the average pore size of the PA hydrogel was around 12 nm. The ribosomes were encapsulated during the rehydration of the predried PA hydrogel particles, which facilitated convective transport induced by expanding the gel network.<sup>45</sup> After the rehydration, the ribosomes were entrapped inside the cell-mimic particles due to the larger size than the hydrogel pores. We also observed that the plasmid templates were encapsulated inside the hydrogel, probably due to both the interaction between the  $\text{Ni}^{2+}$  and the DNA phosphates<sup>46</sup> and the entanglement of the DNA strands with the hydrogel polymer backbone (Fig. S1†).

The expression of non-His-tagged mCherry was performed in the cell-mimic particles to verify the capability of protein expression. A red fluorescence was observed in the cell-mimic particles when the plasmid containing the non-His-tagged mCherry coding gene was encapsulated into the cell-mimic particles (Fig. 2a and b). The SDS-PAGE results (Fig. 2c) confirmed that non-His-tagged mCherry was expressed inside the cell-mimic particles and then diffused out to the surroundings. By contrast, no proteinaceous factors or ribosome bands could be found in the surroundings, indicating that the proteinaceous factors and ribosome of the PURE system remained inside the cell-mimic particles. The non-His-tagged mCherry observed in the surroundings indicated that the protein product freely diffused out of the cell-mimic particles, providing a potential means of communication with nearby cell-mimic particles. The results proved that the cell-mimic particle was (i) a self-maintaining system that kept the proteinaceous factors, ribosome and plasmid template inside the cell-mimic particle; and (ii) an open system that allowed exchange of nutrients, energy, and expression products between the cell-mimic particle and the surroundings.

The expression yield of non-His-tagged eGFP was measured to evaluate the efficiency of the cell-mimic particles. A group of ten cell-mimic particles in 5  $\mu\text{L}$  feeding buffer reached the expression equilibrium after 4 hours, with the final non-His-tagged eGFP concentration in the surrounding buffer at 197  $\mu\text{g mL}^{-1}$ . In the control experiment, we prepared 5  $\mu\text{L}$  feeding buffer with the same composition. The buffer solution also contained the same amount of proteinaceous factors and ribosome of the PURE system as in the combined ten cell-mimic particles. The yield of non-His-tagged eGFP in the solution of

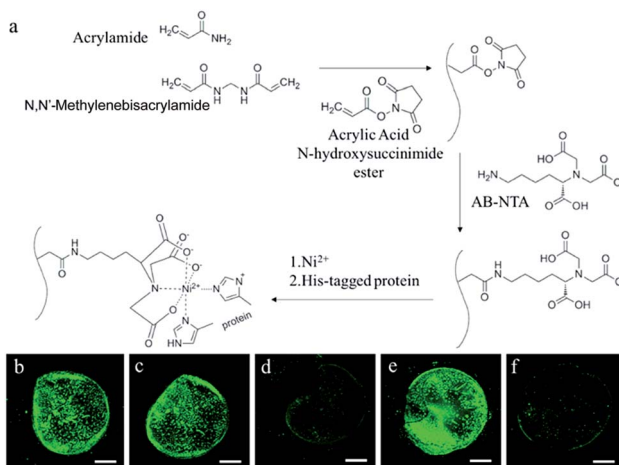


Fig. 1 (a) The schematic of the synthesis of the functionalized polyacrylamide (PA) hydrogel; (b) confocal images of the functionalized PA hydrogel containing the His-tagged eGFP; (c) and (d) confocal images of the same functionalized PA hydrogel as in (b) after washing with water and with imidazole, respectively; (e) and (f) confocal images of the same unfunctionalized PA hydrogel containing the His-tagged eGFP before and after washing with water, respectively. Scale bars in the images are 500  $\mu\text{m}$ .



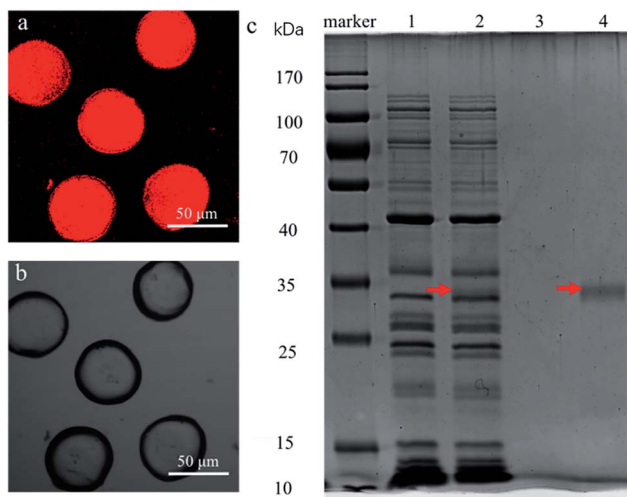


Fig. 2 (a) Confocal images of the cell-mimic particles expressing non-His-tagged mCherry; (b) bright field image of the cell-mimic particles; (c) SDS-PAGE results of the cell-free expression of non-His-tagged mCherry using the PURE system. Lane 1: the PURE system in aqueous solution without the DNA template. Lane 2: PURE system in aqueous solution with the mCherry DNA template. Lanes 3 and 4: the cell-mimic particles' surrounding buffer before and after the mCherry expression, respectively. The mCherry bands were highlighted with red arrows.

the control experiment reached equilibrium after 2 hours, with the final non-His-tagged eGFP concentration of  $87 \mu\text{g mL}^{-1}$ . By comparison, the *in vivo* expression in *E. coli* yielded eGFP with the concentration on the scale of tens of  $\mu\text{g mL}^{-1}$ .<sup>47,48</sup> The results showed that the protein yield and the expression efficiency were higher in the cell-mimic particles than in the aqueous solution and in the *E. coli* cells.<sup>47–49</sup> The high expression efficiency of the cell-mimic particles was an unexpected observation. In *E. coli*, on which the PURE system is based, the transcription and translation processes are coupled, which require a close proximity of ribosome, RNA polymerase, and other related factors. The efficient expression of non-His-tagged eGFP in the cell-mimic particles suggested that the polymer backbone was flexible enough to support the diffusive movement of the immobilized factors and facilitate the coupled transcription and translation processes.<sup>50</sup> The better performance of the cell-mimic particles in protein expression is probably because the proteinaceous factors were confined inside the cell-mimic particles with a much higher local concentration.<sup>27</sup> We expect that smaller or thinner cell-mimic particles with higher surface-area-to-volume ratio will have higher expression yield, as the exchange of nutrients, energy, and expression products by diffusion will take less time.<sup>27</sup>

Next, we tested the capability of long-lived protein expression of the cell-mimic particles. The cell-mimic particles were placed in a microchamber which was connected to the main channel through a side channel (Fig. 3a). Due to the sub-millimeter dimension of the microchannel and the low flow rate, the exchange of nutrients, energy, and expression products between the cell-mimic particles and the solution in the main channel was achieved by diffusion through the side channel. The

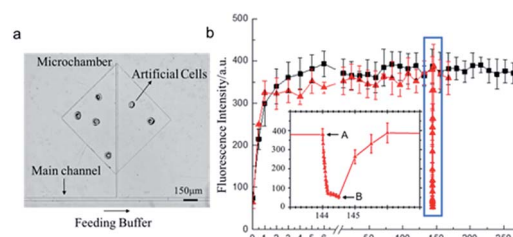


Fig. 3 (a) The microfluidic setup for the continuous protein expression in the cell-mimic particles. (b) The average fluorescence signal from 5 cell-mimic particles during the continuous expression of non-His-tagged mCherry. The black square data points represent the fluorescence signal from the cell-mimic particles continuously fed by the feed buffer at  $37^\circ\text{C}$ . The red triangle data points represent the signal from the control experiment with a brief period of temperature drop. The inset is the blow-up of the rectangular region of the control experiment. Time point A indicates the moment when the temperature was decreased to room temperature to pause the mCherry expression, and time point B indicates the moment when the temperature returned to  $37^\circ\text{C}$  to resume the mCherry expression.

openness of the cell-mimic particles was crucial to the long-lived protein expression in the cell-mimic particles for the efficient energy and nutrient supply and waste discharge. During the experiment, the nutrients and the energy agents continuously diffused into the cell-mimic particles to support the protein expression, while the protein products and by-products diffused out of the cell-mimic particles. When continuously feeding the cell-mimic particles, we observed stable expression of non-His-tagged mCherry for at least 11 days (Fig. 3b). In the control experiment, the temperature was decreased to room temperature to pause the expression. The associated decrease of the fluorescence signal indicated the loss of non-His-tagged mCherry in the cell-mimic particles by diffusion (Fig. S2†). Once the temperature returned to  $37^\circ\text{C}$ , the expression resumed and the fluorescence signal in the cell-mimic particles was recovered (Fig. 3b). We expect the protein expression to continue until the immobilized proteinaceous factors of the PURE system and the ribosomes degrade. The long-lived protein expression of the cell-mimic particles facilitated more complex functions of the cell-mimic particles such as protein expression regulation and gene networks.

The cell-mimic particles were then used to achieve the regulation of the gene expression. *E. coli* RNA polymerase was added to the PURE system to initiate the transcription and translation of the protein LacI, which would impede the transcription of the non-His-tagged mCherry gene by binding with the Lac operator linked to the mCherry gene. When isopropyl  $\beta$ -D-thiogalactopyranoside (IPTG) was added into the feeding buffer, LacI would bind to IPTG, releasing the Lac operator to activate the mCherry expression (Fig. 4a). After the addition of IPTG into the feeding buffer, the mCherry expression level would be enhanced. The mCherry expression level increased with the increase of the IPTG concentration until the IPTG concentration reached  $10 \text{ mM}$  (Fig. 4b). When IPTG was removed from the feeding buffer, the mCherry expression returned to the initial low level as the LacI protein would bind to

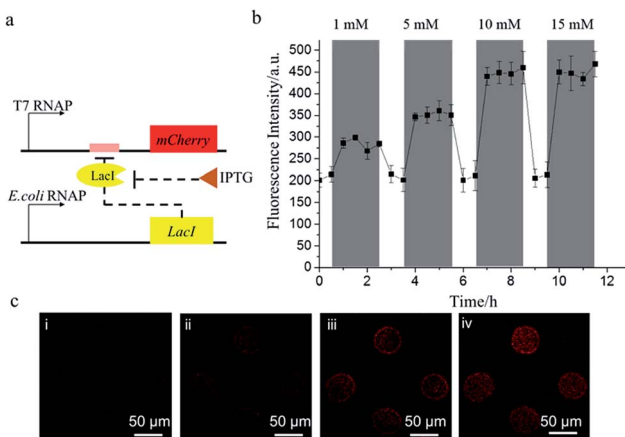


Fig. 4 (a) The schematic of the IPTG regulation process. (b) The change of the *mCherry* expression level due to the IPTG regulation. The gray areas denote the period of the addition of different concentrations of IPTG to the feeding buffer. (c) Confocal microscopy images of cell-mimic particles expressing *mCherry* with the feeding buffer containing (i) no IPTG, (ii) 1 mM IPTG, (iii) 5 mM IPTG, and (iv) 10 mM IPTG.

the Lac operator again. The cell-mimic particles' response to IPTG showed their potential to be a biosensor platform in addition to being a useful cell model for the research of gene networks and cell-cell communication.

We further demonstrated a negative feedback gene oscillator in the cell-mimic particles. With the transcription action of T7 RNA polymerase, protein LacI and non-His-tagged eGFP were expressed simultaneously in the cell-mimic particles. The accumulation of protein LacI would inhibit the expression of eGFP and LacI as a negative feedback, leading to the decreased expression level of LacI and eGFP (Fig. 5a).<sup>51</sup> Once the accumulated LacI diffused out of the cell-mimic particles, the promoters became free of bound LacI and the cycle began anew. As expected, the fluorescence signal of eGFP showed an oscillation, with a period of about 2 minutes (Fig. 5b). The period of the oscillator in the cell-mimic particles was much shorter than the period of the same oscillator in natural cells.<sup>51</sup> The difference is likely because the oscillator period was related to the removal rate of the proteins.<sup>51</sup> In natural cells, the protein products were degraded by catabolic enzymes, while in the cell-mimic particles, the decrease of the protein level was dependent

on the diffusion process, which was much quicker than the degradation process.<sup>51</sup> With the demonstration of the gene oscillator, we expect that cell-mimic particles possess great potential as a platform to test the dynamic behavior of the gene network.

## Conclusions

In conclusion, we built a new type of self-maintaining and self-regulating cell-mimic particle. The prominent features of the cell-mimic particles are the long-lived and efficient protein expression in the particles. The features were achieved through the immobilization of the cell-free transcription and translation system on the polymer backbone of the cell-mimic particles, which rendered the particles capable of continuous uptake of nutrients and energy from the surroundings and the diffusion of the protein expression products out of the particles.

With the long-lived and efficient protein expression, the cell-mimic particles supported the gene regulation and gene circuit engineering. We envision that the cell-mimic particles will also be a useful platform for biosensors such as toehold-based sensors for viruses<sup>52</sup> and for the research of cell-cell communication such as biofilm disruption.<sup>53</sup> In addition, with a coating of a lipid bilayer, the cell-mimic particles provide a potential starting point to the construction of artificial cells and drug delivery vehicles.<sup>54</sup>

## Conflicts of interest

There are no conflicts to declare.

## Acknowledgements

We acknowledge the financial support by the Research Grants Council of Hong Kong (GRF 14303917), The Chinese University of Hong Kong (Direct Grant 4053158), and the Hong Kong Ph.D. Fellowship (H.-W.) from the Research Grants Council of Hong Kong.

## Notes and references

- 1 J. W. Szostak, D. P. Bartel and P. L. Luisi, *Nature*, 2001, **409**, 387–390.
- 2 D. Deamer, *Trends Biotechnol.*, 2005, **23**, 336–338.
- 3 P. L. Luisi, F. Ferri and P. Stano, *Naturwissenschaften*, 2006, **93**, 1–13.
- 4 S. Rasmussen, L. Chen, D. Deamer, D. C. Krakauer, N. H. Packard, P. F. Stadler and M. A. Bedau, *Science*, 2004, **303**, 963–965.
- 5 C. Lartigue, J. I. Glass, N. Alperovich, R. Pieper, P. P. Parmar, C. A. Hutchison III, H. O. Smith and J. C. Venter, *Science*, 2007, **317**, 632–638.
- 6 A. Pohorille and D. Deamer, *Trends Biotechnol.*, 2002, **20**, 123–128.
- 7 C. Chiarabelli, P. Stano and P. L. Luisi, *Curr. Opin. Biotechnol.*, 2009, **20**, 492–497.

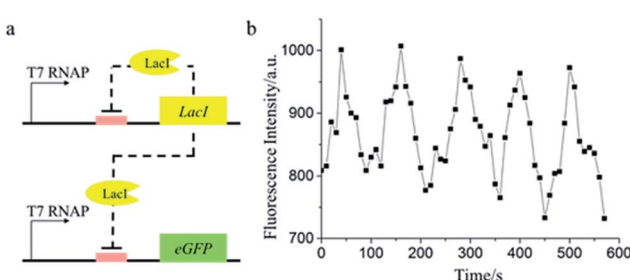


Fig. 5 (a) The schematic of negative feedback oscillation. (b) The fluorescence trajectory of a single cell-mimic particle containing the gene network with negative feedback.



8 C. E. Ashley, E. C. Carnes, G. K. Phillips, D. Padilla, P. N. Durfee, P. A. Brown, T. N. Hanna, J. Liu, B. Phillips, M. B. Carter, N. J. Carroll, X. Jiang, D. R. Dunphy, C. L. Willman, D. N. Petsev, D. G. Evans, A. N. Parikh, B. Chackerian, W. Wharton, D. S. Peabody and C. J. Brinker, *Nat. Mater.*, 2011, **10**, 389–397.

9 Y. Zhang, W. C. Ruder and P. R. LeDuc, *Trends Biotechnol.*, 2008, **26**, 14–20.

10 K. Morigaki and P. Walde, *Curr. Opin. Colloid Interface Sci.*, 2007, **12**, 75–80.

11 J. Liu, A. Stace-Naughton, X. Jiang and C. J. Brinker, *J. Am. Chem. Soc.*, 2009, **131**, 1354–1355.

12 S. Prakash and M. L. Jones, *J. Biomed. Biotechnol.*, 2005, **2005**, 44–56.

13 T. M. S. Chang, *Nat. Rev. Drug Discovery*, 2005, **4**, 221–235.

14 A. S. Spirin, V. I. Baranov, L. A. Ryabova, S. Y. Ovodov and Y. B. Alakhov, *Science*, 1988, **242**, 1162–1164.

15 W. Yu, K. Sato, M. Wakabayashi, T. Nakaishi, E. P. Ko-Mitamura, Y. Shima, I. Urabe and T. Yomo, *J. Biosci. Bioeng.*, 2001, **92**, 590–593.

16 S. M. Nomura, K. Tsumoto, T. Hamada, K. Akiyoshi, Y. Nakatani and K. Yoshikawa, *ChemBioChem*, 2003, **4**, 1172–1175.

17 T. Oberholzer, K. H. Nierhaus and P. L. Luisi, *Biochem. Biophys. Res. Commun.*, 1999, **261**, 238–241.

18 P. M. Gardner, K. Winzer and B. G. Davis, *Nat. Chem.*, 2009, **1**, 377–383.

19 R. Lentini, S. P. Santero, F. Chizzolini, D. Cecchi, J. Fontana, M. Marchioretto, C. Del Bianco, J. L. Terrell, A. C. Spencer and L. Martini, *Nat. Commun.*, 2014, **5**, 4012.

20 K. P. Adamala, D. A. Martin-alarcon, K. R. Guthrie-honea and E. S. Boyden, *Nat. Chem.*, 2016, **9**, 431–439.

21 E. Karzbrun, A. M. Tayar, V. Noireaux and R. H. Bar-Ziv, *Science*, 2014, **345**, 829–832.

22 K. Kurihara, M. Tamura, K. Shohda, T. Toyota, K. Suzuki and T. Sugawara, *Nat. Chem.*, 2011, **3**, 775–781.

23 P. Walde, *BioEssays*, 2010, **32**, 296–303.

24 N.-N. Deng, M. Yelleswarapu, L. Zheng and W. T. S. Huck, *J. Am. Chem. Soc.*, 2017, **139**, 587–590.

25 N. P. Kamat, J. S. Katz and D. A. Hammer, *J. Phys. Chem. Lett.*, 2011, **2**, 1612–1623.

26 M. Li, X. Huang, T.-Y. D. Tang and S. Mann, *Curr. Opin. Chem. Biol.*, 2014, **22**, 1–11.

27 N. Park, S. H. Um, H. Funabashi, J. Xu and D. Luo, *Nat. Mater.*, 2009, **8**, 432–437.

28 M. Bayoumi, H. Bayley, G. Maglia and K. T. Sapra, *Sci. Rep.*, 2017, **7**, 45167.

29 C. Martino and A. J. DeMello, *Interface Focus*, 2016, **6**, 20160011.

30 M. W. Nirenberg and J. H. Matthaei, *Proc. Natl. Acad. Sci. U. S. A.*, 1961, **47**, 1588–1602.

31 E. D. Carlson, R. Gan, C. E. Hodgman and M. C. Jewett, *Biotechnol. Adv.*, 2012, **30**, 1185–1194.

32 T. Sawasaki, T. Ogasawara, R. Morishita and Y. Endo, *Proc. Natl. Acad. Sci. U. S. A.*, 2002, **99**, 14652–14657.

33 A. Zemella, L. Thoring, C. Hoffmeister and S. Kubick, *ChemBioChem*, 2015, **16**, 2420–2431.

34 D. M. Kim and J. R. Swartz, *Biotechnol. Bioeng.*, 1999, **66**, 180–188.

35 Y. Shimizu, A. Inoue, Y. Tomari, T. Suzuki, T. Yokogawa, K. Nishikawa and T. Ueda, *Nat. Biotechnol.*, 2001, **19**, 751–755.

36 H. Niederholtmeyer, V. Stepanova and S. J. Maerkl, *Proc. Natl. Acad. Sci. U. S. A.*, 2013, **110**, 15985–15990.

37 V. Noireaux and A. Libchaber, *Proc. Natl. Acad. Sci. U. S. A.*, 2004, **101**, 17669–17674.

38 D. Gerber, S. J. Maerkl and S. R. Quake, *Nat. Methods*, 2009, **6**, 71–74.

39 B. C. Buddingh' and J. C. M. van Hest, *Acc. Chem. Res.*, 2017, **50**, 769–777.

40 J. Thiele, Y. Ma, D. Foschepoth, M. M. K. Hansen, C. Steffen, H. A. Heus and W. T. S. Huck, *Lab Chip*, 2014, **14**, 2651–2656.

41 D. Yang, S. Peng, M. R. Hartman, T. Gupton-Campolongo, E. J. Rice, A. K. Chang, Z. Gu, G. Q. Lu and D. Luo, *Sci. Rep.*, 2013, **3**, 3165.

42 K.-H. Lee, K.-Y. Lee, J.-Y. Byun, B.-G. Kim and D.-M. Kim, *Lab Chip*, 2012, **12**, 1605–1610.

43 R. L. Schnaar and Y. C. Lee, *Biochemistry*, 1975, **14**, 1535–1541.

44 Z. Han, W. Li, Y. Huang and B. Zheng, *Anal. Chem.*, 2009, **81**, 5840–5845.

45 Y. Li, D. Guo and B. Zheng, *RSC Adv.*, 2012, **2**, 4857–4863.

46 T. Pawłowski, J. Swiatek, K. Gasiorowski and H. Kozłowski, *Inorg. Chim. Acta*, 1987, **136**, 185–189.

47 P. Lu, C. Vogel, R. Wang, X. Yao and E. M. Marcotte, *Nat. Biotechnol.*, 2007, **25**, 117–124.

48 C. Albano, L. Randers-Eichhon, Q. Chang, W. Bentley and G. Rao, *Biotechnol. Tech.*, 1996, **10**, 953–958.

49 Y. Chen, L.-N. Wei and J. D. Muller, *Proc. Natl. Acad. Sci. U. S. A.*, 2003, **100**, 15492–15497.

50 R. A. Sheldon, *Adv. Synth. Catal.*, 2007, **349**, 1289–1307.

51 J. Stricker, S. Cookson, M. R. Bennett, W. H. Mather, L. S. Tsimring and J. Hasty, *Nature*, 2008, **456**, 516–519.

52 S. Slomovic, K. Pardee and J. J. Collins, *Proc. Natl. Acad. Sci. U. S. A.*, 2015, **112**, 14429–14435.

53 R. Lentini, N. Y. Martín, M. Forlin, L. Belmonte, J. Fontana, M. Cornellà, L. Martini, S. Tamburini, W. E. Bentley, O. Jousson and S. S. Mansy, *ACS Cent. Sci.*, 2017, **3**, 117–123.

54 P. F. Kiser, G. Wilson and D. Needham, *Nature*, 1998, **394**, 459–462.

